Biogeosciences Discussions

Title Page

Abstract	Introduction
Conclusions	References
Tables	Figures

Back | Close

Full Screen / Esc

Print Version

Interactive Discussion

EGU

Aggregate structure and stability linked to carbon dynamics in a south Chilean Andisol

D. Huygens[1], P. Boeckx[1], O. Van Cleemput[1], R. Godoy[2], and C. Oyarzún[3]

[1]Laboratory of Applied Physical Chemistry – ISOFYS, Ghent University, Coupure 653, 9000 Gent, Belgium
[2]Institute of Botany, Universidad Austral de Chile, Casilla 567, Valdivia, Chile
[3]Institute of Geosciences, Universidad Austral de Chile, Casilla 567, Valdivia, Chile

Correspondence to: D. Huygens (dries.huygens@ugent.be)

Abstract

The extreme vulnerability of soil organic carbon to climate and land use change emphasizes the need for further research in different terrestrial ecosystems. We have studied the aggregate stability and carbon dynamics in a chronosequence of three different land uses in a south Chilean Andisols: a second growth *Nothofagus obliqua* forest (SGFOR), a grassland (GRASS) and a *Pinus radiata* plantation (PINUS). The aim of this study was to investigate the role of Al as soil organic matter stabilizing agent in this Andisol. In a case study, we linked differences in carbon dynamics between the three land use treatments to physical protection and recalcitrance of the soil organic matter (SOM). In this study, C aggregate stability and dynamics were studied using size and density fractionation experiments of the SOM, δ^{13}C and total carbon analysis of the different SOM fractions, and mineralization measurements. The results showed that electrostatic attractions between and among Al-oxides and clay minerals are mainly responsible for the stabilization of soil aggregates and the physical protection of the enclosed soil organic carbon. Whole soil C mineralization rate constants were highest for SGFOR and PINUS, followed by GRASS. In contrast, incubation experiments of isolated macro organic matter fractions showed that the recalcitrance of the SOM decreased in another order: PINUS > SGFOR > GRASS. We concluded that physical protection of soil aggregates was the main process determining whole soil C mineralization. Land use changes affected soil organic carbon dynamics in this south Chilean Andisol by altering soil pH and consequently available Al.
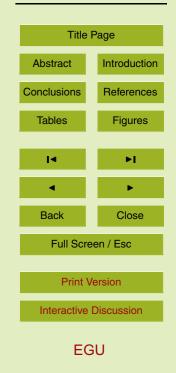
1. Introduction

Andisols develop from volcanic ash and are characterised by a high soil organic matter (SOM) content, good physical properties, and a high anion- and cation exchange capacity (AEC and CEC) (Galindo and Bingham, 1977). Their clay fraction consists mainly of poorly crystalline allophane, imogolite, and oxides and oxyhydroxides of Fe

EGU

Carbon dynamics in a Chilean Andisol

D. Huygens et al.

EGU

and Al (Besoain, 1958). Allophane is a group of clay minerals made up of silica, aluminum, and water in a chemical combination (Parfitt, 1990). In southern Chile (35°–49° S lat), Andisols cover a large part of the surface area of the Central Valley and Andes mountain ranges (FAO-UNESCO, 1971).

5   General overviews of changes in C-stocks after land use conversions are given by Paul et al. (2002) and Guo and Gifford (2002). De Koning et al. (2003) concluded more specific that in Al-rich soils, changes in C-stocks follow a pattern according to land use history and accompanying changes in soil characteristics. Temperate native forests covered most of southern Chile for the last 3000 years, remaining almost intact until

10 the arrival of the Europeans, 450 years ago (Lara et al., 1999). Significant land use changes have taken place in this region (Lara et al., 1999). Today, only 56% (or 10.3 million ha) of this original forest cover remains. Most affected are the *Sclerophyllus* and the *Nothofagus* forest types, with 3 and 30% of the original forest cover remaining, respectively (Lara et al., 1999). On the other hand, grasslands and schrublands have

15 doubled in area, from 2.5 to 5.5 million ha (Lara et al., 1999). New land use types, such as urban areas (55 000 ha), arable lands (2.8 million ha) and forestry plantations (2.1 million ha), now occupy a significant area as well.

Soil organic matter (SOM) has a very complex and heterogeneous composition and is generally mixed or associated with the mineral soil constituents to form soil aggre-

20 gates (Del Galdo et al., 2003). Soil organic matter dynamics are mainly influenced by its recalcitrance and accessibility, and interactions between SOM and soil components (Sollins et al., 1996). Recalcitrance is the inherent molecular level resistance of a molecule to microbial and enzymatic breakdown. Accessibility is the extent to which the location of substrates controls access by microbes, fungi or enzymes. Interactions

25 of organic substrates with organic or inorganic molecules may alter the degradation rate of the substrates (Swanston et al, 2002). Several studies have shown that in aluminum rich soils, such as Andisols, chemical stabilisation is the determining process for carbon accrual (Zunino et al., 1982; Percival et al., 2000). However, the exact role of SOM and Al in the process of chemical stabilization, and which kind of interactions

occurs between the different soil components is not yet fully understood.

The objective of this study was to evaluate the role of Al on carbon dynamics in Chilean Andisols and to investigate C stabilization by electrostatic Al-C binding, and occlusion within soil aggregates. As a case study, we tried to assess the effect of changes in certain physical and chemical soil characteristics – which resulted from the land use conversions – on SOC, physical protection of SOC in aggregates, quality of SOC, and organo-mineral associations. A chronosequence of three different land uses were studied: a second growth *Nothofagus obliqua* forest (SGFOR), a grassland (GRASS), and a plantation of *Pinus radiata* (PINUS).

2. Materials and methods

2.1. Site description and soil sampling

Soil samples were taken in August 2002 near Paillaco, in the Central Valley of southern Chile (40°07 S, 72°51 W). The mean annual precipitation varies from 1600–1800 mm, while mean annual temperature is 10.8°C. All soils were classified as *trumao's* or Andisols, Typic Dysandrepts (Tosso, 1985). They have typical variable electrical charge characteristics (i.e. pH dependent) as a result of their particular clay mineral and humus content (Radcliffe and Gillman, 1985; Nanzyo et al., 1993). A mixture of 1:1 and 2:1 clay minerals (e.g. halloysite, vermiculite, etc.) has been documented in Chilean Andisols as well as the generally observed poorly crystalline minerals (Besoain, 1958, 1969; Galindo and Bingham, 1977; Besoain et al., 2000).

The three sites are all located in close proximity (100 m apart) and were originally all under the same forest vegetation dominated by *Nothofagus obliqua*. Nowadays, only the SGFOR site is still under this original vegetation. The land use of the GRASS and PINUS sites changed 50–100 years ago from second growth *N. obliqua* forest to grassland for agricultural livestock activity. Finally, 16 years ago, a *Pinus radiata* plantation was established on a part of the GRASS site.

Carbon dynamics in a Chilean Andisol

D. Huygens et al.

Title Page

Abstract	Introduction
Conclusions	References
Tables	Figures

◄ | ►

◄ | ►

Back | Close

Full Screen / Esc

Print Version

Interactive Discussion

EGU

The second growth *N. obliqua* forest (SGFOR) has a mean tree height of 35 m, a stand density of 757 ha^{-1} and a canopy cover of 70% during the growing season. The average tree age is 120 years, while mean diameter at breast height equals 42.5 cm. In this forest, the overstorey is dominated by *N. obliqua* (32 m) with a cover of 40%.

5 The understorey (25 m) consists of *Aextoxicon punctatum*, *Persea linque*, *Nothofagus obliqua*, *Eucriphia cordifolia*, *Laurelia sempervirens*, *Nothofagus dombeyi* and *Gevuina avellana* with a cover of 70%. The lower understorey (10 m) is dominated by *Aextoxicon punctatum*. In the shrub stratum (<4 m) *Chusquea quila* and *Raphithamnus spinosus* are dominant.

10 Since the establishment of the pasture, agricultural activities (cattle breeding) have taken place on the GRASS and PINUS sites with an animal density of 1.5–2 cows ha^{-1}. The grassland has a species composition consisting of *Lolium perenne* L. and *Trifolium repens* L., and is ploughed and resown every two years. A mixture of various forms of acidifying fertilizers has been applied yearly on the GRASS site at high levels, though

15 no data were available on the exact fertilizer type or application rate.

On the PINUS site, fertilization was stopped with the establishment of the plantation, 16 years ago. This *P. radiata* monoculture has a mean tree height of 15–18 m, while stand density is around 1500 ha^{-1}.

Sampling was done after selection of representative plots in the three ecosystem

20 sites (land use treatments). In each land use treatment, three sampling plots were selected based on pedological, forestry and ecological experience. Samples originating from a different sampling plot in the same land use treatment were considered as replicates, and were kept separate for later analysis. In each sampling plot, one soil sample has been taken at 0–10, 10–20 and 20–30 cm depth. Thus, in total 27 soil

25 samples were taken. After transport to the laboratory, the recognisable plant material was removed. All soil samples were dried, homogenised and sieved (2 mm) for later analyses. Soil samples were dried in open air to a gravimetric water content of approximately 20%. Volcanic-ash soils can granulate irreversibly when completely dried (Kubota, 1972), and this can affect the subsequent fractionation of SOM. We will refer

EGU

to these partly dried samples using the term "air dried samples".

2.2. Size and density fractionation of SOM

The size fractionation procedure was performed by separately wet sieving a soil sample of 100 g over three sieves (250 μm, 150 μm and 50 μm) with tap water. The suspension passing the bottom size was collected and left about 48 h at room temperature to settle. After settling, the clear solution was removed and the size fraction <50 μm was collected. Four size fractions (2000–250 μm, 250–150 μm, 150–50 μm and <50 μm) were obtained, dried at 40°C for 48 h and homogenised using a planetary ball mill (PM400, Retsch, Germany) for subsequent analysis.

The size fractionation was performed at two different times, using the same procedure: (1) starting from "air dried" soil (slaking) and (2) after an 80 day laboratory incubation experiment (wet sieving of field moist soil) (see below). In the incubation experiment, the soil was exposed to several supplementary disruption processes such as rewetting and mixing of the soils. Using this procedure, the susceptibility of the soil aggregates against disruption processes could be evaluated. The distribution of the soil weight among the different size fractions was expressed using the weighted average diameter (WAD) and could thus be quantified as one single parameter for further statistical analyses. The difference in WAD between the two fractionation experiments can be related to the stability of the soil aggregates. A smaller difference in WAD indicates a higher stability of the soil aggregates.

Density fractionation of the soil organic matter was performed using the method of Meijboom et al. (1995) (Fig. 1). Air dried soil samples (400 g) were wet sieved over two sieves with tap water (top sieve mesh size 250 μm, bottom sieve mesh size 150 μm), until the passing water became clear in order to destroy all macroaggregates >150 μm. Next, the two size fractions retained on the sieves were washed into a bucket and swirled with a jet of water to separate the organic matter (OM) from the mineral fraction by decantation. Swirling and decanting were repeated until no more floating organic matter appeared. The obtained macro organic matter (MOM) from both size frac-

Carbon dynamics in a Chilean Andisol

D. Huygens et al.

EGU

EGU

tions (250–2000 and 150–250 μm) was recombined to be further separated into a light (LF, density <1.13 Mg m^{-3}), intermediate (IF, 1.13 Mg m^{-3}< density <1.37 Mg m^{-3}) and heavy (HF, density >1.37 Mg m^{-3}) fraction by subsequent submersion in two colloidal silica suspensions (Ludox, Dupont, USA) with a respective density of 1.13 Mg m^{-3} and 1.37 Mg m^{-3}. The obtained density fractions were washed with distilled water and dried at 40°C for 48 h.

The C concentrations increase with decreasing density of the fractions (LF > IF > LF). The IF and HF show a higher association of the SOM of these heavier fractions with soil minerals (Hassink, 1995). The LF consists mainly of recognisable plant material in an early stage of decomposition and serves as readily decomposable substrate for the microbial biomass (Six et al., 1999; Solomon et al., 2000).

2.3. Carbon mineralization experiments

The C mineralization experiments consisted out of two different experiments. In a first experiment, whole soil C mineralization was measured. In a second experiment, isolated macro organic matter fractions (LF and HF) were incubated to determine the specific C mineralization of these fractions.

Before starting the whole soil C mineralization experiment, the air dried soil was rewetted and pre-incubated during six days at a temperature of 15°C. Air dried bulk samples were brought to a gravimetric water content of 46% for SGFOR and PINUS, respectively, and 32% for GRASS, corresponding to a water filled pore space of 25% at the bulk density in the field (using a bulk density for all the layers of 0.45 Mg m^{-3} for SGFOR and PINUS, and 0.60 Mg m^{-3} for GRASS (see Table 1) and a soil particle density of 2.65 Mg m^{-3}). As such, a realistic microbial soil activity could be restored. An exact quantity of soil was put in PVC tubes (4.6 cm diameter, 13 cm high) and compressed manually to the corresponding bulk density. The tubes were covered with parafilm, which permits sufficient gas exchange and aeration, but reduced moisture loss. During the entire experiment, the moisture content and temperature were kept constant. Carbon dioxide emission was measured on eight different time points (day 1,

Title Page

Abstract | Introduction

Conclusions | References

Tables | Figures

◄ | ►

◄ | ►

Back | Close

Full Screen / Esc

Print Version

Interactive Discussion

EGU

3, 7, 11, 17, 35, 43 and 62). This was done by putting the PVC-tubes into glass jars, which were closed airtight. The headspace of the glass jars was sampled after 0, 27, 54 and 81 min through a rubber septum. Before sampling, the CO_2 concentration in the headspace was homogenised by repeatedly sucking and re-injecting the headspace.

5 A gas sample of 1 mL was injected into a gas chromatograph (GC-14B, Shimadzu, Japan) (Porapack Q, mesh size 80/100 column specification, electron capture detector (ECD)). The CO_2 concentration was calculated via a linear calibration using a certified CO_2 concentration (1% CO_2 in dry air, Air Liquide, France). Linear regression between the measuring points at 0, 27, 54 and 81 min gave the CO_2 mineralization flux.

10 The incubation of the isolated HF and LF was only performed for SOM originating from the 0–10 cm soil layer of each land use treatment, following the method described by Swanston et al. (2002). For LF, 2.00 g substrate was mixed with 18.00 g inert quartz sand (acid washed, 580–650 μm diameter) in a glass flask. For HF, 5.00 g substrate was mixed with 15.00 g inert quartz sand. A microbial inoculum was added at the

15 beginning of the incubation. A water extract from the mineral soil originating from the same soil layer was used as inoculum source. The inoculum was made by adding distilled water to a wet soil in a 1/1.5 ratio, followed by placing the mixture on a rotary shaker for 30 min. After settling down, 4 mL of the supernatant was added to each flask and the substrate was pre-incubated for two days. During the entire experiment, the

20 inoculated flasks were stored in an incubation room at a constant temperature of 15°C. The CO_2 concentration was measured through a septum in the cap of the flasks after 0, 27, 54 and 81 min and on six different time points (day 1, 3, 7, 11, 17 and 35) with a gas chromatograph (GC-14B, Shimadzu, Japan), using the same method as described above.

25 2.4. Physico-chemical analyses

Measurement of ^{13}C and total C (TC) content in the different soils and SOM fractions was performed using an elemental analyser (ANCA-SL, PDZ-Europa, UK) coupled to an Isotope Ratio Mass Spectrometer (20–20, PDZ Europa, UK). The measured

^{13}C/^{12}C ratios are expressed as δ^{13}C values (‰) vs. the international Vienna Pee Dee Belemnite (VPDB) standard:

$$\delta^{13}\text{C} = \frac{\text{R}_{sample} - \text{R}_{standard}}{\text{R}_{standard}} \cdot 1000 (‰) \tag{1}$$

R$_{sample}$ and R$_{standard}$ refer to the ^{13}C/^{12}C ratio of the measured sample and the standard, respectively. The working standard was flour with a δ^{13}C value of -27.01 ± 0.04‰ vs. VPDB and TC of 39.95 ± 0.40‰ (certified by Iso-Analytical, UK).

A modified procedure of the method described by Schwertmann (1964), using a mixture of ammonium oxalate (0.2 M) and oxalic acid as extractant, was applied for the determination of the extractable aluminum oxalate (Al$_{ox}$), and silicon oxalate (Si$_{ox}$) content. In the absence of light, a soil:solution (1:10) mixture was placed on a rotary shaker for 2 h. A pyrophosphate reagent (0.1 M) was used in soil:solution ratio of 1:10 (shaking time 16 h) for the determination of the pyrophosphate extractable Al content (Al$_{py}$). All supernatants were centrifuged at 3000 rpm for 10 min, filtrated (folded filters, Schleicher & Schüell, Germany) and the Al and Si content of the solutions were determined with, respectively, ICP-OES (Inductive Coupled Plasma – Optical Emission Spectrometry) (VISTA-MPX CCD Simultaneous ICP-OES, Varian, USA), and AAS. Allophane contents were calculated using the formula proposed by Parfitt and Wilson (1985), and later simplified by Mizota and van Reeuwijk (1989):

$$\text{Allophane} = 100\,\text{Si}_{ox} \cdot \left[23.4 - 5.1 \left(\frac{\text{Al}_{ox} - \text{Al}_{py}}{\text{Si}_{ox}} \right) \right] (\%) \tag{2}$$

2.5. Statistical analyses

Statistical analyses were performed using SYSTAT version 10.0 (SPSS, USA). Statistical differences of means (95% significance level) were distinguished using ANOVA (3 replicates) followed by a Duncan's multiple range post-hoc test. Paired samples T-tests were used to determine differences in C mineralization rates between LF and HF

EGU

fractions. Log transformation was used to improve normality and homoscedastisticy in the data when necessary. In case no homogeneity of variance was reached after log transformation, Tamhane's T2 test was used as post-hoc test. Correlations were determined by the "Pearson's correlation factor".

3. Results

3.1. Physico-chemical soil properties

The chemical and physical properties of the soils are listed in Table 1. Averaged over the three soil layers, land use changes significantly affected soil C stocks with +31 and −42% for the conversion from SGFOR to GRASS and GRASS to PINUS, respectively. The N content was highest in GRASS, followed by SGFOR and PINUS. Nitrogen concentrations varied from 0.53 to 0.18 kg m^{-2}. Fertilizer additions on the GRASS site are responsible for the higher N contents in this site. The bulk density was higher in GRASS than in SGFOR and PINUS and is as well a result of agricultural livestock activities. Soil texture was categorized as sandy loam (USDA texture class) for all the land use treatments. The soils in SGFOR and PINUS showed an average pH$_{H2O}$ between 6.1 and 6.7. In contrast, GRASS showed a lower pH$_{H2O}$ (around 5.5). The extractable Al$_{ox}$ and Al$_{py}$ concentrations in the GRASS site were higher than for SGFOR and PINUS, though differences between GRASS and PINUS were not always significant for Al$_{ox}$. Soil pH was negatively correlated with Al$_{ox}$ ($r = -0.45$; $p = 0.02$), and Al$_{py}$ ($r = -0.83$; $p = 0.00$). Allophane contents were for the three soil layers significantly lower for GRASS compared to SGFOR and PINUS.

3.2. Size and density fractionation

The highest weight percentage after the first size fractionation was found in the size fraction 250–2000 μm (Fig. 2). The other size fractions contain smaller amounts of

Carbon dynamics in a Chilean Andisol

D. Huygens et al.

soil weight, varying from 23.1 to 7.0% for all land use treatments. The WAD was not significantly different between the different land use treatments, except for PINUS 20–30 cm where a significant lower value was found (Table 2). TC concentration (%) was not significantly different among the different size fractions in all the sites, with exception of the 0–10 cm layer of SGFOR (Table 3).

The results of the weight distribution of the second size fractionation experiment (after an 80 day incubation period, starting from field moist soil) are shown in Fig. 3. A considerable shift in soil weight towards the finer size fractions could be noticed, which results in a smaller WAD compared to the first fractionation procedure (Table 2). Between land use treatments, GRASS showed the coarsest aggregate distribution but due to relative large standard deviations (on average 50 μm), differences in WAD were only significant for the 20–30 cm layer. As in the first fractionation procedure, the soil carbon concentration did not differ significantly among the different size classes for all land uses, though a few exceptions were observed here (data not shown).

Averaged over the three soil layers, the aggregate stability decreased in the following order: GRASS > PINUS > SGFOR, however only significant differences were observed for the 20–30 cm layer between SGFOR and GRASS (Table 2). The difference in WAD was negatively correlated with the extractable Al_{ox} content of the soil ($r=-0.50$; $p=0.01$), but not with the TC content ($r=-0.18$; $p=0.38$), extractable Al_{py} content ($r=-0.23$; $p=0.25$) or allophane content ($r=0.11$; $p=0.60$) of the soil.

The amounts of MOM are expressed relative to the TC content (i.e. as % of total C) (Table 4). The differences between land use treatments diminished with depth and were only significant between SGFOR, GRASS and PINUS for the 0–10 cm and 10–20 cm layer. The quantities of MOM for the three soil layers, expressed as % of total C, were negatively correlated with the extractable Al_{ox} content of the soil ($r=-0.74$, $p<0.01$).
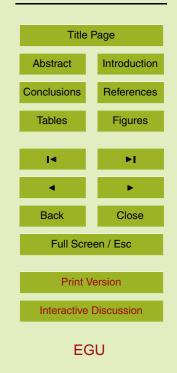
Table 5 shows the complete mass and carbon balance for the 0–10 cm. It was found that the C content of the MOM is only a small fraction of the total C content (2.4%–8.3%) in the soil. Though the concept of the fractionation procedure assumes that

Title Page

Abstract | Introduction

Conclusions | References

Tables | Figures

|◀ | ▶|

◀ | ▶

Back | Close

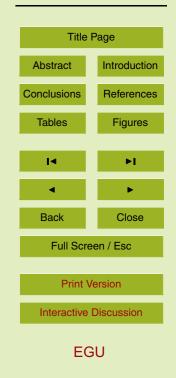Full Screen / Esc

Print Version

Interactive Discussion

EGU

macroaggregates (>150 μm) are broken and the enclosed organic matter is released, still 56–74% of the TC content of the soil was found in the remaining mineral fraction (i.e. the fraction 150–2000 μm, from which the MOM is isolated).

3.3. δ^{13}C signature in size and density fractions

The δ^{13}C values of the whole soil C and the different SOM fractions from the three land use treatments and soil layers are presented in Table 6. Within the different size and density fractions of a certain land use, no significant differences in δ^{13}C value were found. However, a significant difference of 1-2‰ was found between the δ^{13}C value of the size classes and density classes for the different land use treatments, with exception for PINUS 0–10 cm.

3.4. Mineralization experiments

3.4.1. Whole soil C mineralization

The cumulative C mineralization curves were calculated for all land use treatments as shown in Fig. 4 for SGFOR. The linear part of each curve (from day 17 to 62) was used to estimate the potential C mineralization rate via linear regression (Table 7). The differences in potential C mineralization rates between the different land use treatments were significant in the 0–10 cm soil layer: SGFOR > PINUS > GRASS. However, differences between the three land use treatments disappeared gradually with depth. In the 10–20 cm and 20–30 cm layer SGFOR still showed the highest potential mineralization rate, but differences were no longer significant. For all land use treatments, potential C mineralization rates decreased with soil depth. The C mineralization rate constant, which can be used as an indicator of the degradability of the SOM, was calculated by dividing the observed potential C mineralization rate (expressed per gram soil) by the corresponding TC content in each soil layer (Table 7). For the 0–10 cm soil layer, these values varied from 0.029 for SGFOR to 0.023 for PINUS and 0.011 yr^{-1} for GRASS. In

EGU

all soil layers, the decomposability of the SOM was significantly lower for GRASS than for PINUS and SGFOR. The SOM from GRASS showed the highest stability against microbial breakdown.

3.4.2.   Incubation of the isolated MOM density fractions HF and LF

In this procedure, the MOM was isolated by the density separation procedure, through which the physical protection of SOM in soil aggregates was removed (Fig. 1). Especially, the accessibility of the HF has been increased, as this fraction is more associated with soil minerals and components compared to the LF. The LF is mainly present in the soil as free MOM. Only a small fraction is bounded in soil aggregates (Hassink, 1995; Swanston et al., 2002). Potential C mineralization rates and C mineralization rate constants of the isolated density fractions were calculated using the same method as the whole soil C mineralization experiment (Table 8). There, the mineralization rate constants are an indicator of the recalcitrance of the macro organic matter fractions. Statistical analyses showed that the potential C mineralization rates of the LF and HF were significantly different for all land use treatments. The C mineralization rate constants of the LF and HF are significantly different for GRASS, but not for SGFOR and PINUS.

The C mineralization rate constants showed that the MOM from GRASS decomposes fastest. The recalcitrance of the LF decreased in the following order: PINUS > SGFOR > GRASS. For the HF, PINUS showed a higher recalcitrance than GRASS, whereas the value of SGFOR was not significantly different from PINUS and GRASS (Table 8).

4.   Discussion

In a first section of the discussion, we will focus on the interaction of Al, SOM and soil minerals. Al-humus complexes, electrostatic-C binding and aggregate structure

EGU

Carbon dynamics in a Chilean Andisol

D. Huygens et al.

Print Version

Interactive Discussion

EGU

will be evaluated in this Andisol. In a second part, we will make a link between aggregate structure, physical and chemical soil properties and C mineralization experiments. Though land use changes certainly affect C dynamics by differences in C input, and direct effects of accompanying soil disturbances (Guo and Gifford, 2002), we will fo-
5   cus on differences in soil properties between land use treatments, which resulted of changes in land use and land management.

The pH differences between GRASS and both SGFOR and PINUS were significant for all soil layers, and most probably a result of the acidifying fertilizer applications. Under lower pH conditions, Al is more soluble and available for complexation with soil
10 components (Wesselink et al., 1996). Consequently, the extractable Al_{ox} and Al_{py} concentrations in the GRASS site were higher than for SGFOR and PINUS. This might be a result of differences in soil pH between the sites, but this is not certain as the extraction procedure changes the soil pH. In the literature (Bertsch and Bloom, 1996), the extractable Al_{py} content is often related to organically bound Al, while the quantity
15 of poorly ordered amorphous or noncrystalline Al phases plus the organically bound Al would be proportional to Al_{ox}. Though, as stated by Bertsch and Bloom (1996), the extractants are not completely selective for specific phases. Considerable overlap between the forms of Al solubilized by a given extractant exists. Pyrophosphate reagent, for instance, forms strong complexes with Al, that, coupled with the high pH (10), can
20 also remove poorly ordered or non-crystalline Al phases associated with SOM (Bascomb, 1968; McKeague and Schluppi, 1982). This non-crystalline Al may be largely coassociated with organic matter that is released via dispersion of the organic material during the pyrophosphate extraction (McKeague and Schluppi, 1982).

The presence of poorly crystalline Fe- and Al-oxides in Andisols is known to have
25 a stabilizing effect on aggregation upon drying (Schahabi and Schwertmann, 1970). Elliott (1986) and Beare et al. (1994) indicated the disrupting effect of physical disturbance such as dry-wet cycles and variations in moisture content on soil aggregates. This explains the decreased resistance of soil aggregates against applied dispersive forces in the second size fractionation procedure.

The results of the size and density fractionation procedures results showed that the extractable Al_{ox} content in the soil is positively related to the stability of soil aggregates. Thus, if less extractable Al_{ox} is present in the soil, less stable soil aggregates can be formed and relatively more SOM will remain in the more labile MOM pool. Though that the GRASS site is ploughed every two years, the aggregates appear to be most stable in this site. The stronger binding forces involved in the soil aggregation process in GRASS overcome the disruptive effect of ploughing on soil aggregates (Beare et al., 1994; Six et al., 1999).

The MOM fractions that were isolated during the fractionation procedure had a significant lower $\delta^{13}C$ value than the SOM that remained in the mineral fraction. It was indicated that the SOM in the mineral fraction has been more processed than the recent incorporated macro organic matter. The $\delta^{13}C$ value of the OM namely increases as decomposition proceeds (O'Brien and Stout, 1978; Accoe et al., 2002). As the OM enters the soil, it is at first found in the more labile MOM pool. Later, after a certain time of processing, it is shifted towards the more stable fractions, where it is enclosed in stable aggregates. Our results are in contrast to Accoe et al. (2002) where a more gradual shift in $\delta^{13}C$ value among the different density and size classes could be observed, indicating a gradual shift of the SOM towards, firstly, a heavier density and, secondly, finer size class as decomposition occurs. In this study, we could only distinguish two different SOM pools: the MOM and the mineral soil pool. The non-significant differences in the MOM fractions for a soil layer can be explained by the absence of major isotopic enrichments of bulk plant material during the early steps of decomposition in forest soils (Balasdent and Mariotti, 1996; Nadelhoffer and Fry, 1988).

4.1. Aggregate structure in south Chilean Andisols

It is generally accepted that SOM is stabilised by Al in Andisols (e.g. Martin et al., 1982; Zunino et al., 1982). In the literature, two different mechanisms can be found for SOM stabilisation by Al. Firstly, organo-Al complexes would act as binding agents between the aggregates or soil particles, through which the enclosed SOM is protected against

Carbon dynamics in a Chilean Andisol

D. Huygens et al.

Print Version

Interactive Discussion

EGU

microbial breakdown. In organo-Al complexes, SOM is sorbed by allophane through ligand exchange between the carboxyl functional groups of the SOM and the surface hydroxyl groups bonded to Al (Parfitt et al., 1977, 1999; Skjemstad, 1992). Since surface hydroxyls are characteristic for variab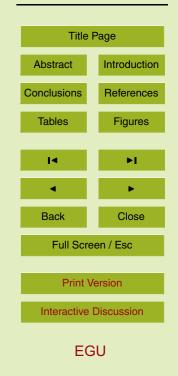le charge surfaces, sorption of negatively charged organics by ligand exchange should be most important in oxide-rich and allophonic soils, such as Andisols (Sollins et al., 1996). In this first case, the mechanism of aggregate hierarchy (Tisdall and Oades, 1982) would be adequate to describe carbon dynamics as SOM (bonded to Al) acts as principal binding agent between soil components.

Secondly, electrostatic attractions could occur between and among Al, Fe and their oxides and clay minerals due to the simultaneous existence of positive and negative charges at field pH (Schofield and Samson, 1954; El-Swaify, 1980; Six et al., 2000b, c; Denef et al., 2002). Thus, here aggregate formation is partly induced by electrostatic interactions and aggregate hierarchy should be less pronounced (Oades and Waters, 1991).

We conceptually tested the occurrence of aggregate hierarchy for the different land use treatments. Three consequences of this theory are: (1) a gradual breakdown of macroaggregates into microaggregates before they dissolve into primary particles, as increasing dispersive energy is applied to the soil (Oades and Waters, 1991), (2) an increase in percentage C concentration with increasing aggregate-size class because large aggregate-size classes are composed of small aggregate-size classes plus organic binding agents (Elliott, 1986), and (3) younger and more labile organic matter is contained in macroaggregates rather than in microaggregates (Elliott, 1986; Puget et al., 1995; Jastrow et al., 1996). Firstly, the fractionation of the soils at two different periods allowed us to test the aggregate stability. A gradual breakdown of macroaggregates into microaggregates could be observed (Figs. 2, 3). It was shown that this breakdown could not be explained by the TC content, allophane content or extractable Al_{py} content of the soil, but by the extractable Al_{ox} content of the soil. In the Al-extraction procedure, only amorphous and poorly crystalline Al-oxides and Al

bound to organic complexes could be isolated (Bertsch and Bloom, 1996). Secondly, the soil C concentration did not differ among the different size classes for a certain land use treatment (Table 3). Thirdly, there were no significant differences in δ^{13}C values among the different size classes for a certain soil (Table 6). The latter indicates that the SOM in the different size fractions is at the same degree of decomposition.

The results of these experiments indicated that organo-Al complexes are probably not the main binding agents between soil aggregates in these Andisols. In small soil particles, organic compounds could be enclosed between soil particles or small aggregates because polyvalent-organic matter complexes form bridges between negative charged 2:1 clay platelets (Six et al., 2000c). However, a further increase in aggregate size would be mainly a result of electrostatic attractions between and among Al and Al-oxides and clay minerals, as documented as well by Schofield and Samson (1954), Violante and Huang (1992) and Denef et al. (2002). Organic matter would only play a minor role in these strong bindings between larger aggregates. As such, large and stable aggregates (cf. mineral fraction) are formed and the enclosed organic matter would experience a high degree of physically protection in these Al-mineral-SOM complexes. These results are in accordance to Denef et al. (2002), who investigated to role of Al and OM in oxide rich soils with a different clay mineralogy. These authors also suggested that the presence of non-crystalline oxides, vermiculites and 1:1 clay minerals in soils leads to very strong interactions between 2:1 and 1:1 clay minerals, oxides and organic matter compounds, and hence high levels of stable macroaggregation with high inputs of OM.

Allophane contents were significantly lower for GRASS than for SGFOR and PINUS. It was indicated that as a result of a lower pH, aluminum was released from allophanic compounds, and resulted in a higher Al content associated with the mineral-SOM complexes. Statistical evidence for this conclusion was found by a strong significant correlation between soil pH and allophane (r=0.74, p=0.00). Increased aluminum release from allophane at decreasing pH was also found by Farmer and Lumsdon (2002). Dahlgren and Saigusa (1994) found in Andisols evidence for the precipitation of re-

Carbon dynamics in a Chilean Andisol

D. Huygens et al.

EGU

EGU

leased Al from allophanic components on soil surfaces, while Walker et al. (1988) found more specifically that soluble Al was adsorbed extremely rapid on common soil minerals such as vermiculite. Violante and Huang (1992) found in OM rich soils that aggregation between soil particles was promoted by increasing Al precipitation. Tama and El-Swaify (1978) stated that soil pH affects the ability of soil particles to aggregate in another important way in variable charge soils. The electrostatic contribution of oxides to aggregate stability is pH dependent and affects the extent of aggregate breakdown at different pH values. In lowering soil pH, the amount of positive charges of the Al-oxides and allophane increases (Espinoza et al., 1975). As such, more electrostatic forces are involved in aggregating soil particles. This indicates that the soil pH could affect aggregate stability. However, in our statistic analyses of the aggregate stability test no significant correlation was found between soil pH and difference in WAD between the two fractionation procedures. Possibly, the sigmoid retention curves, relating the effect of soil pH and positive charges, documented in south Chilean Andisols (Espinoza et al., 1975) might be responsible for the absence of a linear correlation.

4.2. C-mineralization experiments

For the 0–10 cm layer, the whole soil C mineralization rate constant decreased in the following order: SGFOR ≈ PINUS > GRASS. Our values are in accordance to those found in Columbian Andisols by Boudot et al. (1986), who measured a mineralization rate constant of approximately 0.01 yr^{-1} in the 5–20 cm layer. For the incubation of the isolated MOM density fractions, the C mineralization rate constant of GRASS was highest. GRASS SOM showed thus the lowest recalcitrance against microbial breakdown (see further), but however, its SOM physical protection and macroaggregate turnover was highest.

In Andisols, it is known that metal-humus complexes are resistant to microbial decomposition (Juste et al., 1975), and offer as such physical protection against microbial breakdown. Gijsman and Sanz (1998) also investigated the physical protection of macroaggregates in Andisols. After crushing of macroaggregates, these authors ob-

EGU

served a significant increase in CO_2 mineralization compared to intact soil samples. Plante and McGill (2002) indicated that macroaggregate turnover results in the exposure of labile organic matter. Jastrow (1996) found evidence for a relationship between macroaggregate formation and C accrual. Six et al. (2000a) underscored the importance of soil aggregation and more specifically the interactions of SOM and aggregate dynamics in controlling C-sequestration in soils.

In our study, the C mineralization rate constants (SGFOR $\approx$ PINUS > GRASS) showed an opposite trend as the aggregate stability. It was indicated that aggregate stability affects the C mineralization process in Andisols. The latter was confirmed by the significant correlation between the whole soil C mineralization rate constants and the difference in WAD (r=0.39, p=0.04). The lower C mineralization rate constants in GRASS are probably a result of the stabilization of the SOM by aluminum in Andisols (see above). Further statistical evidence for this conclusion was found in a strong negative and significant correlation between the mineralization rate constant and Al_{ox} content (r=−0.68, p=0.00). Percival et al. (2000) also indicated that the C stabilization by Al can lead to exceptionally slow soil C turnover.

5. Conclusions

It can be concluded that either by electrostatic bridges between Al-oxides and clay minerals, and dissolution of Al from allophanic compounds, physico-chemical stabilization of the SOM occurs. It is important to mention that Al compounds are mainly bound directly onto clay minerals via electrostatic attractions. However, as clay minerals are closely associated with organic matter compounds, stable Al-mineral-humus complexes can be formed. It was also indicated that this process of aggregate stabilization has an important effect on C mineralization.

In this study, land use conversion from a second growth forest (SGFOR) to a grassland (GRASS) showed, indirectly, a positive effect on C stabilization in the soil. In Andisols, soil management practices may affect the stability of Al-mineral-humus com-

plexes via the soil pH and consequently the available Al content. Due to the reduced pH, more stable soil aggregates could be formed in GRASS and a higher physical protection of its SOC was reached. This was indicated by a smaller difference in WAD between the two fractionation experiments, and a smaller MOM fraction. Apparently, this positive pH effect on soil aggregation was even able to overcome the disruptive effect of frequent ploughing in GRASS. Moreover, though the recalcitrance of the SOM in GRASS was lowest, physical protection in soil aggregates resulted in a reduced C mineralization in this site. Percival et al. (2000) also indicated that land use changes from forest to grassland in Andisols can alter C dynamics, especially if a change in the stability of the Al-mineral-humus complexes occurs.

References

Accoe, F., Boeckx, P., Van Cleemput, O., Hofman, G., Hui, X., Bin, H., and Guanxiong, C.: Characterization of soil organic matter fractions from grassland and cultivated soils via C content and δ^{13}C signature, Rap. C. Mass., 16, 2157–2164, 2002.

Balasdent, J. and Mariotti, A.: Measurement of soil organic matter turnover using 13C natural abundance, in: Mass spectrometry of soils, edited by: Boutton, T. W. and Yamasaki, S., Marcel Dekker, New York, 1996.

Bascomb, C. L.: Distribution of pyrophosphate extractable iron and organic carbon, J. Soil Sci., 19, 251–268, 1968.

Beare, M. H., Hendrix, P. F., and Coleman, D. C.: Water-stable aggregates and organic matter fractions in conventional and no-tillage soils, Soil Sci. So., 58, 777–786, 1994.

Bertsch, P. M. and Bloom, P. R.: Aluminum, in: Methods of soil analysis Part 3- Chemical methods, edited by: Sparks, D. L., SSSA Book Series, SSSA, Madison, 1996.

Besoain, E. M.: Mineralogia de las arcillas de algunos suelos volcánicos de Chile, Agr. Téc., 18, 110–165, 1958.

Besoain, E. M.: Clay mineralogy of volcanic ash soils, Panel of Volcanic ash soils in Latin America, Soil B.1.1-B.1.16., Turrialba, Costa Rica, 1969.

5　Besoain, E. M., Peralta, M. P., and Massaro, S. M.: Mineraloga y genesis de algunas suelos de cenizas volcánicas de Chiloé continental, Chile, Agr. Téc., 60, 127–153, 2000.

Boudot, J. P., Bel Hgadj, B. A., and Chone, T.: Carbon mineralization in Andosols and aluminium-rich highland soils, Soil Biol. B., 18, 457–461, 1986.

Dahlgren, R. A. and Saigusa, M.: Aluminum release rates from allophanic and nonallophanic
10　andosols, Soil Sci. Pl., 40, 125–136, 1994.

de Koning, G. H. J., Veldkamp, E., and López-Ulloa, M.: Quantification of carbon sequestration in soils following pasture to forest conversion in northwestern Ecuador, Global Biol., 17, 4, 9.1–9.12, doi:10.1029/2003GB002099, 2003.

Del Galdo, I., Six, J., Peressotti, A., and Cotrufo, M. F.: Assessing the impact of land-use
15　change on soil C sequestration in agricultural soils by means of organic matter fractionation and stable C isotopes, Gl. Change B., 9, 1204–1213, 2003.

Denef, K., Six, J., Merckx, R., and Paustian, K.: Short-term effects of biological and physical forces on aggregate formation in soils with different clay mineralogy, Plant Soil, 246, 185–200, 2002.

20　Elliott, E. T.: Physical and mechanical properties of Oxisols, in: Soils with variable charge, edited by: Theng, B. K. G., Offset Publications, Palmerston North, 303–324, 1986.

Espinoza, W., Gast, R. G., and Adams, R. S. J.: Charge characteristics and nitrate retention by two Andepts from south-central Chile, Soil Sci. So., 39, 842–846, 1975.

FAO-UNESCO: Soil map of the world, Volume IV, South America, UNESCO, Paris, 1971.

25　Farmer, V. C. and Lumsdon, D. G.: A re-interpretation of 'Aluminium solubility mechanisms in moderately acid Bs horizons of podzolized soils' by Gufstafsson et al., Eur. J. So. Sc., 53, 671–673, 2002.

Galindo, G. G. and Bingham, T.: Homovalent and heterovalent cation exchange equilibria in soils with variable surface charge, Soil Sci. So., 41, 833–866, 1977.

30　Gijsman, A. J. and Sanz, J. I.: Soil organic matter pools in a volcanic-ash soil under fallow or cultivation with applied chicken manure, Eur. J. So. Sc., 49, 427–436, 1998.

Guo, L. B. and Gifford, R. M.: Soil carbon stocks and land use change: a meta analysis, Gl. Change B., 8, 345–360, 2002.

**Carbon dynamics in a
Chilean Andisol**

D. Huygens et al.

EGU

Hassink, J.: Density fractions of soil macroorganic matter and microbial biomass as predictors of C and N mineralization, Soil Biol. B., 27, 1099–1108, 1995.

Jastrow, J. D.: Soil aggregate formation and the accrual of particulate and mineral-associated organic matter, Soil Biol. B., 28, 665–676, 1996.

Juste, C., Delas, J., and Langon, M.: Comparison de la stabilité biologique de différents humates métalliques, Comptes Rendus Acad. Sci., 281, 1685–1688, 1975.

Kubota, T.: Aggregate formation of allophonic soils: effect of drying on the dispersion of the soils, Soil Sci. Pl., 18, 79–87, 1972.

Lara, A., Solari, M. E., Rutherford, P., Thiers, O., Tracaman, R., Molina, R., Prieto, R., and Montory, C.: Cobertura de la vegetación original de la Ecoregión de los bosques valdivianos en Chile hacia 1550, Informe Técnico. Proyecto FB 49-WWF/Universidad Austral de Chile, Valdivia, Chile, 1999.

Martin, J. P., Zunino, H., Peirano, P., Caiozzi, M., and Haider, K.: Decomposition of 14C-labilled lignins, model humic acid polymers and fungal melanins in allophanic soils, Soil Biol. B., 14, 289–293, 1982.

McKeague, J. A. and Schluppi, P. A.: Changes in concentration of iron and aluminum in pyrophosphate extracts of soil and composition of sediment extraction from soil resulting from ultracentrifugation in relation to spodic horizon criteria, Soil Sci., 134, 265–270, 1982.

Meijboom, F. W., Hassink, J., and Van Noordwijk, M.: Density fractionation of soil macroorganic matter using silica suspensions, Soil Biol. B., 27, 1109–1111, 1995.

Mizota, C. and van Reeuwijk, L. P.: Clay mineralogy and chemistry of soils formed in volcanic material in diverse climatic regions, Soil Monogr. 2, Int. Soil Reference and Information Centre, Wageningen, The Netherlands, 1989.

Nadelhoffer, K. and Fry, B.: Controls on natural nitrogen-15 and carbon-13 abundances in forest soil organic matter, Soil Sci. So., 52, 1633–1640, 1988.

Nanzyo, M., Dahlgren, R. A., and Shoji, S.: Chemical characteristics of volcanic ash soils, in: Volcanic ash soils: Genesis, properties and utilization, edited by: Shoji, S., Nanzyo, M., and Dahlgren, R. A., Developments in Soil Science 21, Elsevier, Amsterdam, the Netherlands, 1993.

Oades, J. M. and Waters, A. G.: Aggregate hierarchy in soils, Aust. J. Soil, 29, 815–828, 1991.

O'Brien, B. J. and Stout, J. D.: Movement and turnover of soil organic matter as indicated by carbon isotope measurements, Soil Biol. B., 10, 309–317, 1978.

Parfitt, R. L.: Allphane in New Zealand – a review, Aust. J. Soil, 28, 343–360, 1990.

Carbon dynamics in a Chilean Andisol

D. Huygens et al.

Title Page

Abstract | Introduction

Conclusions | References

Tables | Figures

|◄ | ►|

◄ | ►

Back | Close

Full Screen / Esc

Print Version

Interactive Discussion

EGU

Parfitt, R. L. and Wilson, A. D.: Estimation of allophane and halloysite in three sequences of volcanic soils, New Zealand, in: Volcanic soil, edited by: Caldas, E. F. and Yaalon, D. H., CATENA suppl. 7, Catena, Braunschweig, Germany, 1985.

Parfitt, R. L., Fraser, A. R., and Farmer, V. C.: Adsorption on hydrous oxides, III. Fulvic acid and humic acid on goethite, gibbsite and imogolite, J. Soil Sci., 28, 289–296, 1977.

Parfitt, R. L., Yuan, G., and Theng, B. K. G.: A 13C-NMR study of the interactions of soil organic matter with aluminium and allophane in podzols, Eur. J. So. Sc., 50, 695–700, 1999.

Paul, K. I., Polglase, P. J., Nyakuengama, J. G., and Khanna, P. K.: Change in soil carbon following afforestation, Forest Ecol., 168, 241–257, 2002.

Percival, H. J., Parfitt, R. L., and Scott, N.: Factors controlling soil carbon levels in New Zealand grasslands: Is clay content important?, Soil Sci. So., 64, 1623–1630, 2000.

Plante, A. F. and McGill, W. B.: Intraseasonal soil macroaggregate dynamics in two contrasting field soils using labeled tracer spheres, Soil Sci. So., 66, 1285–1295, 2002.

Puget, P., Chenu, C., and Balasdent, J.: Total and young organic matter distributions in aggregates of silty cultivated soils, Eur. J. So. Sc., 46, 449–459, 1995.

Radciffe, D. J. and Gillman, G. P.: Surface charge characteristics of volcanic ash soils from the southern highlands of Papua New Guinea, in: Volcanic soil, edited by: Caldas, E. F. and Yaalon, D. H., CATENA suppl. 7., Catena, Braunschweig, Germany, 35–46, 1985.

Schahabi, S. and Schwertmann, U.: Der Einfluss von Synthetischen Eisenoxides auf die Aggregation zweier Lussbodenhorizonte, Z. Pflanzenernaehr. Bodenkd., 125, 193–204, 1970.

Schofield, R. K. and Samson, H. R.: Flocculation of kaolinite due to the attraction of oppositely charged crystal faces, Faraday Dis., 18, 135–145, 1954.

Schwertmann, U.: Differenzierung der Eisenoxide des Bodens durch Photochemische Extraction mit saurer Ammoniumoxalate Lösung, Z. Pflanzenernaehr. Bodenkd., 105, 194–202, 1964.

Six, J., Elliott, E. T., and Paustian, K.: Aggregate and soil organic matter dynamics under conventional no-tillage systems, Soil Sci. So., 63, 1350–1358, 1999.

Six, J., Elliott, E. T., and Paustian, K.: Soil macroaggregate turnover and microaggregate formation: a mechanism for C sequestration under no-tillage agriculture, Soil Biol. B., 32, 2099–2103, 2000a.

Six, J., Elliott, E. T., and Paustian, K.: Soil structure and soil organic matter: II. A normalized stability index and the effect of mineralogy, Soil Sci. So., 64, 1042–1049, 2000b.

Six, J., Paustian, K., Elliott, E. T., and Combrink, C.: Soil structure and soil organic matter: I.

EGU

Distribution of aggregate size classes and aggregate associated carbon, Soil Sci. So., 64, 681–689, 2000c.

Skjemstad, J. O.: Genesis of Podzols on coastal dunes in southern Queensland: III. The role of aluminium-organic complexes in profile development, Aust. J. Soil, 30, 645–665, 1992.

5 Sollins, P., Homann, P., and Caldwell, B. A.: Stabilization and destabilization of soil organic matter: mechanisms and controls, Geoderma, 74, 65–105, 1996.

Solomon, D., Lehmann, J., and Zech, W.: Land use effects on soil organic matter properties of chromic Luvisols in semi-arid northern Tanzania: carbon, nitrogen, lignin and carbohydrates, Agr. Eco. Env., 78, 203–213, 2000.

10 Swanston, C. W., Caldwell, B. A., Homann, P. S., Ganio, L., and Sollins, P.: Carbon dynamics during a long-term incubation of separate and recombined density fractions from seven forest soils, Soil Biol. B., 34, 1121–1130, 2002.

Tama, K. and El-Swaify, S. A.: Charge, colloidal, and structural stability relationships in oxidic soils, in: Modification of soil structure, edited by: Emerson, W. W., Bond, R. D., and Dexter,

15 A. R., John Wiley & Sons, Chicester, 41–52, 1978.

Tisdall, J. M. and Oades, J. M.: Organic matter and water-stable aggregates in soils, J. Soil Sci., 33, 141–163, 1982.

Tosso, J.: Suelos volcánicos de Chile, Instituto de Investigaciones Agropecuarias, Santiago, Chile, 1985.

20 Violante, A. and Huang, P. M.: Effect of tartaric acid and pH on the nature and physicochemical properties of short-range ordered aluminum precipitation products, Clay. Clay M., 40, 462–469, 1992.

Walker, W. J., Cronan, C. S., and Patterson, H. H.: A kinetic-study of aluminum adsorption by aluminosilicate clay-minerals, Geoch. Cos. A., 52, 55–62, 1988.

25 Wesselink, L. G., van Breemen, N., Mulder, J., and Janssen, P. H.: A simple model of soil organic matter complexation to predict the solubility of aluminium in acid forest soils, Eur. J. So. Sc., 47, 373–384, 1996.

Zunino, H., Borie, F., Aguilera, S., Martin, J. P., and Haider, K.: Decomposition of 14C labeled glucose, plant and microbial products and phenols in volcanic ash-derived soils of Chile, Soil

30 Biol. B., 14, 37–43, 1982.

Carbon dynamics in a Chilean Andisol

D. Huygens et al.

EGU

EGU

Table 1. Chemical and physical properties of the second growth forest (SGFOR), grassland (GRASS) and plantation (PINUS) for the 0–10, 10–20 and 20–30 cm soil layer (standard deviations between brackets). Significant differences ($p<0.05$) between land use treatments within one soil depth layer are indicated by different letters.

Soil layer	Land use class	pH_{H2O}	ρ_b	Al_{ox}	Al_{py}	Si_{ox}	Allophane	TC		TN		C/N
cm			Mg m^{-3}		%			kg C m^{-2}	%	kg N m^{-2}	%	
0–10	SGFOR	6.1^a	0.42	2.03^b	0.64^b	0.96	6.00^a	5.8^{a,b}	13.9^a	0.31^b	0.74^b	18.9
	GRASS	5.7^b	0.60	2.12^a	1.11^a	0.81	5.22^b	6.7^a	11.1^b	0.53^a	0.89^a	12.5
	PINUS	6.2^a	0.45	2.23^a	0.63^b	0.91	6.46^a	4.3^b	9.4^c	0.31^b	0.68^b	13.8
10–20	SGFOR	6.3^a	0.44	2.36^b	0.54^b	1.14	6.99^a	4.0^b	9.3^b	0.23^b	0.55^b	16.9
	GRASS	5.4^b	0.46	2.41^a	1.05^a	0.85	5.57^b	4.8^b	10.5^a	0.37^a	0.81^a	13.0
	PINUS	6.4^a	0.46	2.44^a	0.61^b	0.91	6.63^a	3.3^a	7.1^c	0.26^b	0.56^b	12.7
20–30	SGFOR	6.3^a	0.52	2.29^b	0.43^b	1.18	7.59^a	3.4^b	6.4^b	0.21^b	0.40^b	16.1
	GRASS	5.8^b	0.60	2.34^a	1.07^a	0.90	5.75^b	5.8^a	9.8^a	0.44^a	0.73^a	13.4
	PINUS	6.7^a	0.47	2.22^b	0.39^b	1.02	7.19^a	2.4^b	5.1^b	0.18^b	0.39^b	13.1

ρ_b = Bulk density
Al_{ox} = Ammonium oxalate extractable Al content
Al_{py} = Pyrophosphate extractable Al content
Si_{ox} = Ammonium oxalate extractable Si content
Allophane = Estimated allophane content
TC = Total carbon content
TN = Total nitrogen content

Carbon dynamics in a Chilean Andisol

D. Huygens et al.

Table 2. Distribution of the soil weight according to the size fraction in Fig. 2 and Fig. 3, expressed as weighted average diameter (WAD), of the first and sec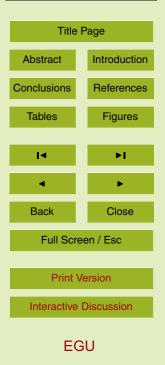ond fractionation procedure, and difference in WAD between the two fractionation procedures for the three soil layers of the second growth forest (SGFOR), grassland (GRASS), and plantation (PINUS). Significant differences ($p<0.05$) between land use treatments are indicated by different letters.

	0–10 cm			10–20 cm			20–30 cm		
	SGFOR	GRASS	PINUS	SGFOR	GRASS	PINUS	SGFOR	GRASS	PINUS
WAD first fractionation procedure (μm)	786^A	788^A	790^A	794^A	760^A	758^A	739^A	785^A	647^B
WAD second fractionation procedure (μm)	511^A	662^A	572^A	522^A	590^A	585^A	565^B	720^A	526^B
Difference in WAD (μm)	275^A	126^A	218^A	273^A	170^A	173^A	174^A	65^B	$120^{A,B}$

Carbon dynamics in a Chilean Andisol

D. Huygens et al.

EGU

Table 3. Carbon concentrations (%) for the soil layers of the second growth forest (SGFOR), grassland (GRASS), and plantation (PINUS). Significant differences ($p<0.05$) between aggregate size classes for a certain land use treatment and soil depth are indicated by different letters.

Aggregate size class	Carbon concentration (%)								
	0–10 cm			10–20 cm			20–30 cm		
	SGFOR	GRASS	PINUS	SGFOR	GRASS	PINUS	SGFOR	GRASS	PINUS
250 μm–2000 μm	$14.1_{a,b}$	11.1_a	9.3_a	9.0_a	10.5_a	7.1_a	6.6_a	9.8_a	5.2_a
150 μm–250 μm	14.6_a	11.1_a	9.8_a	8.8_a	10.6_a	6.9_a	6.3_a	9.9_a	5.0_a
50 μm–150 μm	14.8_a	10.7_a	9.9_a	9.3_a	10.5_a	7.2_a	6.7_a	9.7_a	5.2_a
<50 μm	12.2 b	11.0_a	8.4_a	8.1_a	10.6_a	6.8_a	6.1_a	9.6_a	4.8_a

EGU

Table 4. Percentage of total C of the macro organic matter fractions (MOM) for the second growth forest (SGFOR), grassland (GRASS) and plantation (PINUS). Significant differences under the same soil depth are indicated by different letters.

Soil depth	% of total C		
	SGFOR	GRASS	PINUS
cm	%		
0–10	8.3^A	2.4^C	5.0^B
10–20	2.8^B	1.6^C	3.6^A
20–30	3.8^A	1.1^B	3.4^A

EGU

Table 5. Weight, C-concentration, and % of total C of the different SOM fractions for the second growth forest (SGFOR), grassland (GRASS) and plantation (PINUS) for the 0–10 cm soil layer. Significant differences (p<0.05) between land use treatments are indicated by different letters.

	Weight ($g\,kg^{-1}$ soil)			C-concentration ($g\,C\,kg^{-1}$ fraction)			% of total C (%)		
	SGFOR	GRASS	PINUS	SGFOR	GRASS	PINUS	SGFOR	GRASS	PINUS
Whole soil	1000	1000	1000	139^A	111^B	94^C			
Size and density fractions MOM	31.5^A	8.6^C	14.4^B	366^A	309^B	$325^{A,B}$	8.3^A	2.4^C	5.0^B
Mineral fraction (150–2000 μm)	738^A	756^A	749^A	108^A	109^A	90^B	56.4^B	74.4^A	71.5^A
50–150 μm	152^A	130^A	143^A	148^A	107^B	99^B	16.7^A	12.5^A	15.0^A
<50 μm	91^A	104^A	93^A	122^A	110^B	84^C	7.9^B	10.3^A	$8.3^{A,B}$
Sum of the fractions							89.5^A	99.6^A	99.7^A

MOM = Macro organic matter (>150 μm)

EGU

Table 6. δ^{13}C values (‰) of the different density and size fractions for the second growth forest (SGFOR), grassland (GRASS) and plantation (PINUS). Significant differences (p<0.05) between soil organic matter fractions are indicated by different letters.

	δ^{13}C								
Fraction	0–10 cm			10–20 cm			20–30 cm		
	SGFOR	GRASS	PINUS	SGFOR	GRASS	PINUS	SGFOR	GRASS	PINUS
	‰								
Whole soil	−27.2	−26.7	−27.8	−26.4	−26.8	−26.7	−26.2	−26.7	−26.4
Macro organic matter	−28.3^b	−28.7^b	−29.2^b	−27.7^b	−27.8^b	−28.2^{b,c}	−27.7^b	−27.5^b	−28.2^b
HF	−28.4^b	−28.8^b	−29.1^{b,c}	−27.8^b	−27.9^b	−27.9^b	−27.7^b	−27.5^b	−28.0^b
IF	−28.3^b	−28.8^b	−29.4^{b,c}	−27.9^b	−27.7^b	−28.4^c	−27.9^b	−27.6^b	−28.3^b
LF	−28.3^b	−28.6^b	−29.2^b	−27.7^b	−27.8^b	−28.2^{b,c}	−27.7^b	−27.5^b	−28.3^b
Size fractions									
250 µm–2000 µm	−27.2^a	−26.7^a	−27.9^a	−26.4^a	−26.8^a	−26.7^a	−26.3^a	−26.7^a	−26.4^a
150 µm–250 µm	−27.2^a	−26.7^a	−27.9^{a,c}	−26.4^a	−26.8^a	−26.7^a	−26.2^a	−26.7^a	−26.3^a
50 µm–150 µm	−27.1^a	−26.6^a	−27.7^{a,c}	−26.4^a	−26.8^a	−26.7^a	−26.2^a	−26.7^a	−26.3^a
<50 µm	−27.2^a	−26.7^a	−27.7^a	−26.4^a	−26.8^a	−26.7^a	−26.1^a	−26.6^a	−26.2^a

HF = Heavy density fraction (density <1.13 Mg m^{-3})
IF = Intermediate density fraction (1.13 Mg m^{-3}< density <1.37 Mg m^{-3})
LF = Light density fraction fraction (density >1.37 Mg m^{-3})

EGU

Table 7. Potential C mineralization rates and decomposition rate constants for the second growth forest (SGFOR), grassland (GRASS) and plantation (PINUS) for 0–10 cm, 10–20 cm and 20–30 cm soil layer. Significant differences between land use treatments ($p<0.05$) are indicated by different letters.

Land use class	Potential mineralization rate			Mineralization rate constant		
	0–10 cm	10–20 cm	20–30 cm	0–10 cm	10–20 cm	20–30 cm
	$g\ CO_2\text{-}C\ m^{-2}\ d^{-1}$			yr^{-1}		
SGFOR	0.495^a	0.192^a	0.142^a	0.029^a	0.017^a	0.018^a
GRASS	0.196^c	0.092^a	0.087^a	0.011^b	0.005^b	0.005^b
PINUS	0.266^b	0.135^a	0.087^a	0.023^a	0.015^a	0.014^a

Table 8. Potential mineralization rates and mineralization rate constants of the light (LF) and heavy (HF) density fraction for the second growth forest (SGFOR), grassland (GRASS) and plantation (PINUS). Significant differences ($p<0.05$) are indicated by different letters (upper case letters between LF and HF, lower case letters between land use treatments).
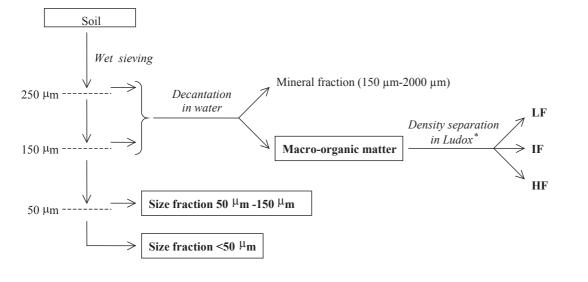
Land use class	Potential mineralization rate		Mineralization rate constant	
	LF	HF	LF	HF
	mg CO_2-C kg^{-1} fraction d^{-1}		yr^{-1}	
SGFOR	131.2^A_a	$59.7^B_{a,b}$	0.120^A_b	$0.090^A_{a,b}$
GRASS	137.4^A_a	73.0^B_a	0.151^A_a	0.106^B_a
PINUS	74.7^A_b	37.6^B_b	0.071^A_c	0.060^A_b

*Ludox : silica suspensions with different density

Fig. 1. Scheme of the density fractionation of SOM; LF = light density fraction (density $<1.13\,\mathrm{Mg\,m^{-3}}$), IF = intermediate density fraction ($1.13\,\mathrm{Mg\,m^{-3}}<$ density $<1.37\,\mathrm{Mg\,m^{-3}}$), HF = heavy density fraction (density $>1.37\,\mathrm{Mg\,m^{-3}}$). (Adapted from Accoe et al., 2002.)

Fig. 2. Distribution of the soil weight over the different size classes (2000–250 μm, 250–150 μm, 150–50 μm, and <50 μm) after the first fractionation procedure (starting from "air-dried" soil) for the second growth forest (SGFOR), grassland (GRASS) and plantation (PINUS) and for the three soil layers (0–10 cm, 10–20 cm, and 20–30 cm).

EGU

Fig. 3. Distribution of the soil weight over the different size classes (2000–250 μm, 250–150 μm, 150–50 μm, and <50 μm) after the second fractionation procedure (starting from field moist soil) for the second growth forest (SGFOR), grassland (GRASS) and plantation (PINUS) and for the three soil layers (0–10 cm, 10–20 cm, and 20–30 cm).

EGU

Fig. 4. Evolution of the cumulative C mineralization for the second growth forest (SGFOR) for the 0–10 cm, 10–20 cm and 20–30 cm soil layer (day 1 to day 62) (error bars indicate plus/minus one standard deviation), and linear regression of the curves (from day 17 to day 62).